Geomech. Geophys. Geo-energ. Geo-resour. (2023) 9:7
https://doi.org/10.1007/s40948-023-00560-0

ORIGINAL ARTICLE

A modified three-dimensional Hoek–Brown criterion for intact rocks and jointed rock masses

Xiangcheng Que · Zhende Zhu · Zihao Niu · Shu Zhu · Luxiang Wang

Received: 29 August 2022 / Accepted: 21 November 2022

Abstract Accurate description of the failure strength behaviors of rock materials, including intact rocks and jointed rock masses, is essential for engineering design and construction. First, a novel three-dimensional (3D) version of the Hoek–Brown (HB) criterion for intact rocks is proposed in this paper. A stress weighting factor n is used in this criterion to describe the effects of intermediate and minimum principal stresses. The proposed 3D version is validated using six sets of polyaxial test data, and its prediction effect is compared with that of five other existing 3D criteria. Results show that the proposed criterion exhibits the smallest prediction error for most rock types. The fitted n is closely correlated to both the partial correlation factors of intermediate and minimum principal stresses. Then, an empirical relationship $m_b(\beta)$ between the material parameter m_b and joint dip angle β is developed to apply the proposed criterion to jointed rock masses. The prediction performance of the proposed empirical relation and three other existing expressions for the m_b of six jointed rock masses at different dip angles is compared, and the proposed relation exhibits the best. The performance of the proposed criterion with empirical relation $m_b(\beta)$ is also verified with nine sets of conventional and true triaxial test data. Results indicate that the predicted strengths are in agreement with the test data. The expression form of the established relation $m_b(\beta)$ can also accurately describe the variation in the m_b value with dip direction α.

Article Highlights

- To quantitatively describe the effects of intermediate and minimum principal stresses, a novel three-dimensional version of the Hoek–Brown criterion for intact rocks is proposed
- An empirical relationship $m_b(\beta$ between the material parameter m_b and joint dip angle β is developed to apply the proposed 3D criterion to jointed rock masses
- Relationships between the weighting factor n in the proposed criterion and the partial correlation factors of intermediate and minimum principal stresses are established

Keywords Three-dimensional Hoek–Brown criterion · Strength · Intact rock · Jointed rock mass · Empirical parameter · Dip angle

Supplementary Information The online version contains supplementary material available at https://doi.org/10.1007/s40948-023-00560-0.

X. Que · Z. Zhu · Z. Niu (✉) · S. Zhu · L. Wang
Key Laboratory of Ministry of Education of Geomechanics and Embankment Engineering, Hohai University, Jiangsu 210098, Nanjing, China
e-mail: 180404010010@hhu.edu.cn

X. Que · Z. Zhu · Z. Niu · S. Zhu · L. Wang
Jiangsu Research Center for Geotechnical Engineering, Hohai University, Jiangsu 210098, Nanjing, China

Published online: 14 February 2023

1 Introduction

The study of the strength behaviors of rock materials under three-dimensional (3D) stress conditions is always a difficult and challenging field. To determine the failure strength of intact rocks and rock masses, numerous strength criteria have been developed (Hoek et al. 1992; Li et al. 2022; Wu et al. 2017; Zhu and Shao 2020). The Hoek–Brown (HB) strength criterion based on the statistical analysis of polyaxial test data is widely used in geotechnical engineering and has been gradually developed to create a relatively complete system (Chen et al. 2021; Gao et al. 2019; Hoek and Brown 1980; Li et al. 2021). The required empirical parameters are related to uniaxial strength behaviors, mineral compositions and structural characteristics of rocks (Hoek et al. 1992). Because this strength criterion can describe the inherent nonlinear failure of rock materials, it is useful in related engineering applications (Merifield et al. 2006; Yang et al. 2018). However, the factor of intermediate principal stress σ_2 is not reflected in the original HB criterion, and many studies (Gong et al. 2019; Zhang et al. 2019, 2022) have illustrated the influence of σ_2 on rock failure. Mogi (1971) conducted high triaxial compression tests on Mizuho trachyte and Dunhan dolomite and revealed the critical effect of σ_2 on rock strength. Takahashi and Koide (1989), Ma and Haimson (2016), Gao et al. (2018), Du et al. (2020) and other scholars reached similar conclusions by performing true triaxial tests on different types of rock.

Thus, developing a 3D version of the HB criterion that reflects the role of σ_2 is vital to understand the strength characteristics of rock materials under 3D stress conditions. Pan and Hudson (1988) elevated the original two-dimensional (2D) HB strength criterion to a 3D version with a circular envelope in the π-plane. Singh et al. (1998) replaced the minimum principal stress σ_3 in the power-law term with $(\sigma_2+\sigma_3)/2$ to realize the three-dimensionalization of the generalized HB (GHB) criterion. Priest (2005) established a new 3D version by combining the Drucker–Prager (DP) criterion (Drucker and Prager 1952) and the GHB strength criterion (Hoek et al. 1992) and reduced it to a simplified version with higher prediction accuracy. Jiang and Zhao (2015) summarized the relationships between the stress invariants of multiple 3D HB criteria and proposed a unified expression and a modified 3D HB criterion. However, the existing 3D HB strength criteria cannot directly or clearly describe the influence of σ_2 and σ_3 on the failure strength of rock materials, and their complex expressions are inconvenient for engineering applications. Therefore, it is crucial to establish a 3D HB strength criterion that is simple in expression and can quantitatively describe the effects of σ_2 and σ_3.

The existing 3D and original 2D HB criteria are primarily used to characterize the failure of intact rocks. Directly using them to explore the failure and strength properties of the jointed rock mass will produce significant errors and cannot reflect the strong joint orientation dependence (Zhang 2008). Many studies (Colak and Unlu 2004; Nasseri et al. 2003; Wen et al. 2021) have demonstrated the differences in the empirical parameter m_b in the HB criterion corresponding to different inclination angles, and a marginal deviation in m_b will lead to large predicted errors. Accurate determination of m_b at different dip angles is a crucial factor in solving the strength parameters of jointed rock mass. Hoek et al. (1992), Tien and Kuo (2001), Lee and Pietruszczak (2008) and other scholars (Ismael and Konietzky 2019; Saroglou and Tsiambaos 2008) successively proposed the relationships $m_b(\beta)$ between the empirical parameter m_b and inclination angle β, and then developed the HB criterion to grasp the strength characteristics of the jointed rock mass under conventional triaxial stress states. Existing empirical equations describe the simple monotonic or quadratic function relationship between m_b and β, and are not suitable for all types of jointed rock masses. Therefore, seeking a universal variation law and establishing an accurate empirical relation $m_b(\beta)$ is critical. It is also necessary to combine this empirical relationship with a reliable 3D HB strength criterion to effectively determine the true triaxial failure strength properties of a jointed rock mass.

In this study, a new 3D expression of HB criterion was first established for intact rocks. To reflect the effects of σ_2 and σ_3 on the rock strength, a weighting factor n was introduced into the 3D criterion, and σ_3 in the power-law term was replaced by $(n\sigma_2+\sigma_3)/(n+1)$. The proposed 3D version was verified using true triaxial test results, and the prediction accuracy was compared with that of five

other 3D HB criteria. Results show the least deviation between the predicted strengths of the proposed criterion and the test values, and the overall prediction effect is superior to the other five. Then, a new empirical relation $m_b(\beta)$ was established to apply the proposed 3D HB criterion to jointed rock masses. The proposed empirical relation $m_b(\beta)$ can describe the monotonic or quadratic function relationship between the parameter m_b and the dip angle β, and also achieves good fitting on the similar periodic variation of m_b. Thus, the proposed 3D HB criterion has good prediction accuracy for the polyaxial strength values of jointed rock masses. The modified 3D HB criterion in this study achieves good predictions and exhibits potential in related engineering applications.

2 Failure criteria for intact rocks

2.1 Existing 3D HB strength criteria

To describe the nonlinearity between the maximum principal stress σ_1 and the minimum principal stress σ_3 of intact rocks, Hoek and Brown (1980) presented the well-known HB strength criterion:

$$\sigma_1 = \sigma_3 + \sigma_{ci}\left(m_i\frac{\sigma_3}{\sigma_{ci}} + 1\right)^{0.5} \tag{1}$$

where σ_{ci} is the failure strength under uniaxial stress, and m_i is the material parameter.

The HB criterion has since been continuously improved while being widely used. Hoek et al. (1992) developed the GHB criterion that can be applied to rock masses with poor quality:

$$\sigma_1 = \sigma_3 + \sigma_{ci}\left(m_b\frac{\sigma_3}{\sigma_{ci}} + s\right)^{a} \tag{2}$$

where m_b, s, and a are the empirical parameters of rock mass. For intact rock, s and a are set equal to 1 and 0.5, respectively.

Because both the original and generalized HB criteria overlook the role of σ_2, the true 3D strength behavior cannot be clearly described. Pan and Hudson (1988) first established a novel 3D criterion, which expresses the relation between the first stress invariant I_1 and second deviatoric stress invariant J_2:

$$\frac{3}{\sigma_{ci}}J_2 + \frac{\sqrt{3}}{2}m_i\sqrt{J_2} - m_i\frac{I_1}{3} = s\sigma_{ci} \tag{3}$$

where the specific expressions of I_1 and J_2 are

$$I_1 = \sigma_1 + \sigma_2 + \sigma_3 \tag{4}$$

$$J_2 = \frac{\left(\sigma_1-\sigma_2\right)^2 + \left(\sigma_2-\sigma_3\right)^2 + \left(\sigma_3-\sigma_1\right)^2}{6} \tag{5}$$

Singh et al. (1998) replaced σ_3 in the power-law term with $(\sigma_2+\sigma_3)/2$ to realize the three-dimensionalization of the GHB criterion:

$$\sigma_1 = \sigma_3 + \sigma_{ci}\left(m_b\frac{\sigma_2+\sigma_3}{2\sigma_{ci}} + s\right)^{a} \tag{6}$$

By combining the GHB and the DP criteria, Priest (2005) established a comprehensive 3D version and developed a simplified expression that performs better than the comprehensive version. The specific expression of the simplified Priest criterion is

$$\begin{aligned}\sigma_1 = {} & 3\left[\mu\sigma_2 + (1-\mu)\sigma_3\right] \\ & + \sigma_{ci}\left[m_b\frac{\mu\sigma_2 + (1-\mu)\sigma_3}{\sigma_{ci}} + s\right]^{a} - \left(\sigma_2+\sigma_3\right)\end{aligned} \tag{7}$$

where μ is an empirical parameter reflecting the influence of σ_2, and its value ranges between 0 and 1.

Jiang and Zhao (2015) summarized a unified relationship between I_1 and J_2 by analyzing the GHB, Singh, Pan–Hudson, Priest and other strength criteria and proposed a relatively simple version:

$$\frac{1}{m_b\sigma_{ci}^{1/a-1}}\left(\sqrt{3J_2}\right)^{1/a} + \frac{2\cos\left(\pi/3-\theta_L\right)}{\sqrt{3}}\sqrt{J_2} - \frac{I_1}{3} = \frac{s\sigma_{ci}}{m_b} \tag{8}$$

where θ_L is the Lode angle.

2.2 Proposed 3D HB strength criterion

Neglecting the role of σ_2 is a deficiency of the GHB criterion. Both the σ_2 and σ_3 affect the rock failure strength characteristics, but in different

proportions. Mogi (1967) also pointed out that the enhancement of the failure strength is affected by σ_2 to a certain extent and developed an empirical function between $(\sigma_1\text{-}\sigma_3)/2$ and $(\sigma_1+\eta\sigma_2+\sigma_3)/2$. η is an effect weighting factor for σ_2. Based on this, we initially considered adopting the $\eta\sigma_2+\sigma_3$ to replace the σ_3 in the power-law term of GHB criterion, thereby establishing a new 3D version. However, when $\sigma_2=\sigma_3$, η must be equal to 0 if the 3D version is to be reduced to the 2D HB criterion. Therefore, a modified 3D HB criterion was developed to describe the effects of σ_2 and σ_3 on rock mass strength:

$$\sigma_1 = \sigma_3 + \sigma_{ci}\left[m_b\frac{n\sigma_2+\sigma_3}{(n+1)\sigma_{ci}} + s\right]^a \tag{9}$$

where n is the stress weighting factor, ranging from 0 to 1. In this criterion, $(n\sigma_2+\sigma_3)/(n+1)$ is used to replace σ_3 in the power-law term. The weighting factor n before σ_2 and the coefficient 1 before σ_3 are interchangeable, and the effects of σ_2 and σ_3 reflected by the proposed criterion are relative. When $\sigma_2=\sigma_3$, the proposed 3D version is automatically converted to the GHB criterion. Equation (9) can be rewritten as follows:

$$\sigma_1 = \sigma_3 + \sigma_{ci}\left[m_b\frac{p\sigma_2+q\sigma_3}{\sigma_{ci}} + s\right]^a \tag{10}$$

where p and q are the empirical parameters for evaluating the influence of σ_2 and σ_3, respectively. p equals $n/(n+1)$ and varies from 0 and 0.5, and q equals $1/(n+1)$ and varies from 0.5 and 1. Compared with the simple Priest criterion (Eq. (7)), Eq. (10) is a more simplified form, and the ranges of the empirical parameters μ and p are different. Mogi (1967) noted that the influence of σ_2 on the failure strength is smaller than that of σ_3; thus, the range of the empirical parameter p set in this study is more reasonable. For intact rocks, Eq. (9) is rewritten as

$$\sigma_1 = \sigma_3 + \sigma_{ci}\left[m_i'\frac{n\sigma_2+\sigma_3}{(n+1)\sigma_{ci}} + 1\right]^{0.5} \tag{11}$$

where m_i' is the empirical coefficient in the proposed criterion.

In the principal stress space, Eq. (9) is expressed by the stress invariants and the Lode angle as

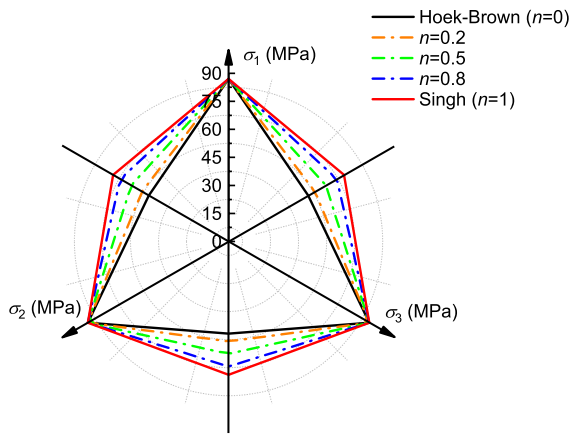

Fig. 1 Failure envelopes in the π-plane of the proposed 3D criterion at $I_1=100$ MPa for sandstone with $\sigma_{ci}=32$ MPa, $m_i=26$, $s=1$, and $a=0.5$

$$F(I_1,J_2,\theta_L) = \sigma_{ci}\left[\frac{m_bI_1}{3\sigma_{ci}} + 2m_b\sqrt{J_2}\,\frac{n\cos\left(\theta_L-\frac{2\pi}{3}\right)+\cos\left(\theta_L+\frac{2\pi}{3}\right)}{\sqrt{3}(n+1)\sigma_{ci}} + s\right]^a - 2\sqrt{\sigma_{ci}}\cos\left(\theta_L-\frac{\pi}{6}\right) \tag{12}$$

To demonstrate the failure envelopes in the π-plane for different weighting factors n, Eq. (12) was applied to sandstone (Du et al. 2020) at $I_1=100$ Mpa. From the expressions of the proposed and other existing 3D versions, it can be seen that Eq. (9) becomes Eq. (2) (2D HB criterion) and Eq. (9) (Singh criterion) at $n=0$ and 1, respectively. Then, both the HB criterion and the Singh criterion were applied to sandstone. As shown in Fig. 1, the cross-sectional shape of Eq. (12) in the π-plane is an irregular hexagon. For different n, the failure strength values are the same at $\sigma_2=\sigma_3$. As n increases from 0 to 1, the envelope gradually expands outward, and the strength at $\sigma_1=\sigma_2$ increases. When n is taken to the minimum value of 0, the role of σ_2 is neglected, and the envelope of the proposed strength criterion is identical to the HB criterion. When n is equal to the maximum value 1, the effects of σ_2 and σ_3 are considered the same, and the envelope of the proposed strength criterion coincides with that of the Singh criterion. Therefore, the Singh and

Table 1 Summary of triaxial test datasets for jointed rock masses

Rock type	Number of data	References
Mizuho trachyte	31	Mogi (1971)
Dunhan dolomite	53	Mogi (1971)
Westerly granite	44	Haimson and Chang (2000)
KTB amphibolites	40	Chang and Haimson (2000)
Coconino sandstone	48	Ma and Haimson (2016)
Sandstone	30	Du et al. (2020)

the GHB criteria can be regarded as the upper and lower bounds of the proposed criterion, respectively.

2.3 Validation of the proposed 3D HB criterion

Six test datasets (Table 1 or Online Resource 1) were adopted to prove the accuracy of the proposed criterion in predicting the failure strength of intact rocks. The selected test data covers uniaxial compression ($\sigma_2=\sigma_3=0$), biaxial compression ($\sigma_1>\sigma_2>\sigma_3=0$), conventional triaxial compression ($\sigma_1>\sigma_2=\sigma_3$), true triaxial compression ($\sigma_1>\sigma_2>\sigma_3\neq 0$), and triaxial tension ($\sigma_1=\sigma_2>\sigma_3$) test results.

Nonlinear regression fitting was performed using the curve fitting tool in the MATLAB software. After selecting the data set, the fitting function was set according to requirements in the custom equations window. The values of parameters in the expression were obtained by the nonlinear least square method. s and a equal 1 and 0.5, respectively, and σ_{ci} represents the uniaxial compression strengths of the six rocks. The calibration parameters m_i', n, p and q for these six intact rocks are listed in Table 2. The relative error percentage (AAREP) and the root mean squared logarithmic error (RMSLE) were employed to evaluate the accuracy of predictions. The specific expressions are

$$\mathrm{AAREP}=\frac{1}{N}\sum_{i=1}^{N}\left|\frac{\sigma_{1,\mathrm{pred}}-\sigma_{1,\mathrm{test}}}{\sigma_{1,\mathrm{pred}}}\right|\times 100\% \tag{13}$$

$$\mathrm{RMLSE}=\sqrt{\frac{1}{N}\sum_{i=1}^{N}\left[\log\left(\sigma_{1,\mathrm{test}}+1\right)-\log\left(\sigma_{1,\mathrm{pred}}+1\right)\right]^2} \tag{14}$$

where $\sigma_{1,\mathrm{test}}$ is the test value of σ_1; $\sigma_{1,\mathrm{pred}}$ is the predicted value of σ_1; N is the data number. The value of AAREP or RMLSE close to 0 demonstrates a better prediction. Table 2 also shows the calculated error measures for the six rocks. Figure 2 shows the best fits of the proposed 3D criterion to the test results.

Table 2 and Fig. 2 show that the proposed criterion can accurately estimate the failure strengths of six intact rocks under different stress states. The weighting factors n of the six rocks are all small. The Dunhan dolomite has the largest n, indicating that the σ_2 dependence of Dunhan dolomite is higher than that of other rocks. The calculated empirical parameter p is approximately 3.26 to 21.22 times q, indicating that the influence of σ_3 is greater than that of σ_3.

To demonstrate the superiority and accuracy of the proposed criterion, the HB, Pan–Hudson, Singh, Priest, and Jiang–Zhao criteria were also adopted to evaluate the failure strength of these six rocks. s, a, and σ_{ci} are the inherent parameters and experimental results of intact rocks, and they are the same as those used in the proposed criterion. The m_i' values in Table 2 are only used in the proposed strength criterion. The m_i values in other existing strength criteria are the respective fitting results with the experimental data. The error measure AAREP and RMLSE values for the six strength criteria are summarized in Fig. 3, and these criteria are ranked according to their prediction accuracy.

Table 2 Calibration results of the proposed 3D HB criterion for six intact rocks

Rock type	σ_{ci} (MPa)	m_i'	n	p	q	AAREP (%)	RMLSE (10^{-2})
Mizuho trachyte	99.13	12.17	0.135	0.119	0.881	3.291	1.814
Dunhan dolomite	257	11.59	0.307	0.235	0.765	3.865	2.114
Westerly granite	201	44.26	0.110	0.099	0.901	4.688	2.598
KTB amphibolites	165	41.34	0.094	0.086	0.914	7.397	4.663
Coconino sandstone	56.1	26.85	0.047	0.045	0.955	7.626	4.010
Sandstone	32.1	26.07	0.214	0.176	0.824	6.501	3.666

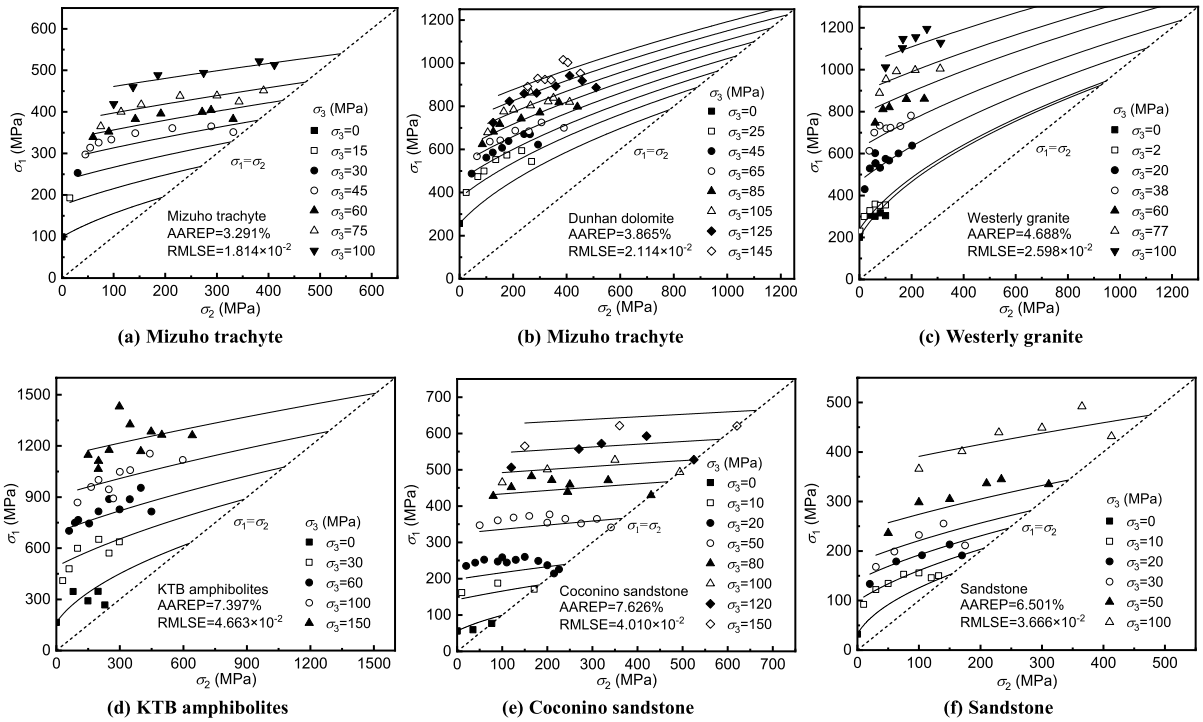

Fig. 2 Best fitting of the proposed criterion to the polyaxial test data

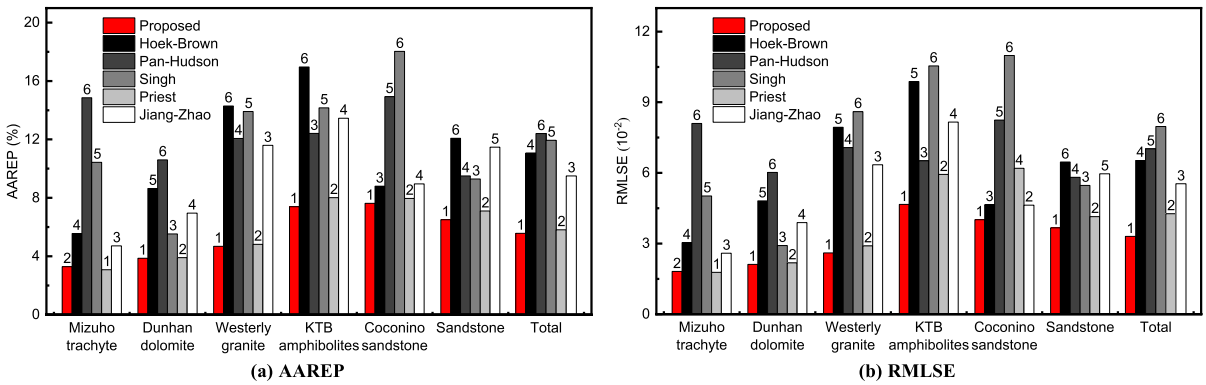

Fig. 3 Error measures of the six criteria for six intact rock types

For the Mizuho trachyte, the simple Priest criterion performs best, with AAREP and RMLSE of 3.080% and 1.781×10^{-2}, respectively. AAREP and RMLSE of the proposed criterion are 3.291% and 1.814×10^{-2}, respectively, indicating a prediction that is not significantly different to the Priest criterion. For the other five rocks, the proposed criterion works better than the other five strength criteria. This is because the stress weighting factor n in the proposed criterion can be adjusted according to the impacts of σ_2 and σ_3, thus improving its predictive ability. The Priest strength criterion also has an empirical parameter μ that describes the role of σ_2. However, the adjustable range of μ is not as accurate as the range of the stress weighting factor n in the proposed criterion, and cannot reflect the fact that the influence capacity of σ_3 is

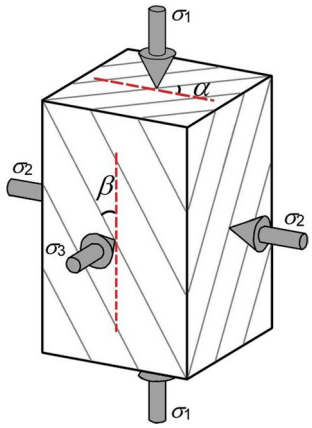

Fig. 4 Relationship between the joint plane and the three principal stress directions

greater than that of σ_2. For the total data of these six rocks, the proposed strength criterion performs best, followed by the simple Priest criterion, Jiang–Zhao, HB, Pan–Hudson, and Singh criteria. The prediction produced by the Singh criterion is worse than the HB criterion because the weighting factor n in the Singh criterion equals 1, overestimating the effect of σ_2. The HB criterion ignores the σ_2 and sets n to 0, which is closer to the calibration results of n in Table 2. The Pan–Hudson criterion achieves poor prediction accuracies and cannot be simplified to the original HB criterion in three-dimensional tension ($\sigma_1 = \sigma_2$) and compression states ($\sigma_2 = \sigma_3$). Overall, the proposed 3D version can describe the failure strength behavior well by adjusting the stress weighting factor n and quantitatively evaluate the impacts of σ_2 and σ_3 on the rock failure.

3 Failure criteria for jointed rock masses

3.1 Existing empirical relations for parameter m_b

In some studies (Ma et al. 2020; Zhang 2008), the 3D strength criteria for intact rocks were used to estimate the failure strength parameters of jointed rock masses, but this cannot describe the high joint directional dependence of the strength behaviors, and the resulting predictions are poor. When establishing the 3D criterion for jointed rock masses, the joint orientation is an important consideration (Singh et al. 2018), including the dip direction α and dip angle β (Fig. 4).

The dip angle β is the primary consideration in the previous true triaxial test study of jointed rock masses (Feng et al. 2019; Zhang et al. 2012; Zhao et al. 2021), and there is a lack of test data considering the comprehensive effect of α and β. Therefore, the existing modified HB criteria (Hoek et al. 1992; Lee and Pietruszczak 2008; Ismael and Konietzky 2019) for jointed rock masses only considers the single factor of β, and the effect of σ_2 is neglected. The empirical parameter m_b of the jointed rock mass is related to the dip angle of the joint plane (Colak and Unlu 2004), thus the original 2D HB criterion is rewritten as

$$\sigma_1 = \sigma_3 + \sigma_{cj}\left[m_b(\beta)\frac{\sigma_3}{\sigma_{cj}} + 1\right]^{0.5} \tag{15}$$

where $m_b(\beta)$ is the empirical parameter m_b at a certain angle of β, and σ_{cj} is the uniaxial compression strength at a certain angle of β. By combining the HB strength criterion expression of Eq. (15), some scholars established the empirical relations $m_b(\beta)$ to predict the strength parameters of anisotropic rock masses. Hoek et al. (1992) first derived an empirical relationship between m_b and β:

$$\frac{m_b(\beta)}{m_b(0°)} = 1 - k_1 \exp\left[-\left(\frac{\beta - k_2}{k_3 + \beta k_4}\right)^4\right] \tag{16}$$

where $m_b(0°)$ is m_b when the dip angle is 0°, and k_1, k_2, k_3, and k_4 are constant terms.

From Jaeger's strength criterion (Jaeger 1960), Tien and Kuo (2001) developed another empirical relation:

$$\frac{m_b(\beta)}{m_b(0°)} = \frac{1}{1 + l\sin^2\beta \cdot \cos^2\beta} \tag{17}$$

where l is a constant term.

Also, Lee and Pietruszczak (2008) established a 3D HB criterion to analyze the rock strength anisotropy, and the relationship between m_b and β is

$$m_b(\beta) = t_1 - t_2 \exp\left[t_3\left(1 - 3\cos^2\beta\right)\right] \tag{18}$$

where t_1, t_2, and t_3 are constant terms.

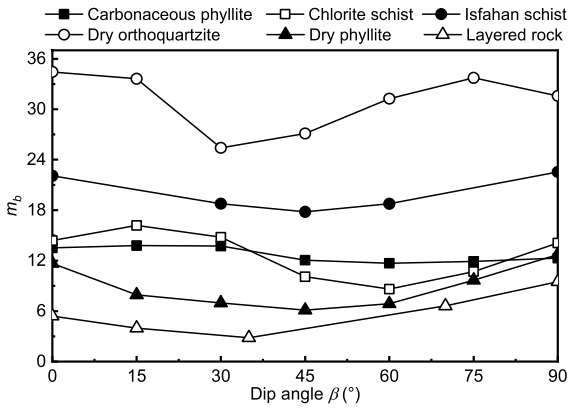

Fig. 5 Variation in the m_b value with dip angle β

3.2 Proposed empirical relation for parameter m_b

To seek the relationship between the empirical parameter m_b and the dip angle β, six triaxial test datasets (Table 3 or Online Resource 2) of jointed rock masses were adopted. Combining Eq. (15), the variations in the m_b value with dip angle β are plotted in Fig. 5.

Figure 5 indicates that the variations in Isfahan schist, dry phyllite, and layered rock show marked quadratic function relationships, and the m_b of carbonaceous phyllite, chlorite schist, and dry orthoquartzite exhibit similar periodic function relationships with dip angle β. The m_b values corresponding to different β were calculated using the existing empirical relations (Eqs. (16)–(18)). Results show that Eqs. (16) and (18) exhibit a monotonic function in the range of $\beta = 0°$–$90°$, while Eq. (17) is a quadratic function symmetric about $\beta = 45°$. Therefore, none of these three empirical relations accurately describe the variation of m_b with the dip angle, particularly for the similar periodic variation curves shown in Fig. 5.

According to the variations in the parameter m_b with the dip angle β shown in Fig. 5, the following empirical function was established:

$$m_b(\beta) = A + B\cos(w \cdot \beta) + C\sin(w \cdot \beta) \tag{19}$$

where A, B, C, and w are constant terms.

Combining Eqs. (11) and (19), the proposed 3D HB criterion is rewritten as the following expression so that it can be applied to the jointed rock masses:

$$\sigma_1 = \sigma_3 + \sigma_{cj}\left[m_b(\beta)\frac{n\sigma_2 + \sigma_3}{(n+1)\sigma_{cj}} + 1\right]^{0.5} \tag{20}$$

In the established 3D criterion Eq. (20) for jointed rock masses, the impacts of σ_2 and joint orientation can be considered concurrently. Because the true triaxial datasets of jointed rock masses considering both α and β are lacking, the proposed strength criterion assumes that the α is fixed and only the β is considered.

3.3 Validation of the proposed empirical relation $m_b(\beta)$ and 3D HB criterion

First, the proposed empirical relation $m_b(\beta)$ and the 3D HB criterion were verified using the six conventional triaxial test datasets listed in Table 3. At this time, $\sigma_2 = \sigma_3$ and Eq. (20) becomes Eq. (15). m_b in Fig. 5 are fitted with Eq. (19), and the calculated values of each constant term are shown in Table 4. The prediction effects of the proposed empirical relationship are evaluated by AAREP and RMLSE. From Table 4, the established empirical relation $m_b(\beta)$ achieves good prediction accuracies for the empirical parameters m_b of six jointed rock masses, and the maximum AAREP and RMLSE are 3.014% and 1.367×10^{-2}, respectively. To demonstrate the

Table 3 Summary of triaxial test datasets for jointed rock masses

Rock type	β (°)	Number of data	References
Carbonaceous phyllite	0, 15, 30, 45, 60, 75, 90	42	Singh et al. (1989)s
Chlorite schist	0, 15, 30, 45, 60, 75, 90	42	Nasseri et al. (2003)
Isfahan schist	0, 30, 45, 60, 90	15	Fehimifar (2004)
Dry orthoquartzite	0, 15, 30, 45, 60, 75, 90	35	Kumar (2006)
Dry phyllite	0, 15, 30, 45, 60, 75, 90	35	Kumar (2006)
Layered rock	0, 15, 35, 70, 90	30	Zhang et al. (2012)

Table 4 Calibration results of the proposed empirical relation $m_b(\beta)$ for six jointed rock masses

Rock type	*A*	*B*	*C*	*w*	AAREP (%)	RMLSE (10^{-2})
Carbonaceous phyllite	12.721	0.801	-0.849	-3.396	1.389	0.687
Chlorite schist	12.426	1.926	-3.367	-3.999	1.789	0.863
Isfahan schist	20.447	1.782	-1.799	3.072	0.612	0.272
Dry orthoquartzite	30.116	4.370	1.201	5.017	2.445	1.298
Dry phyllite	32.637	-21.160	-15.950	0.875	3.014	1.367
Layered rock	7.008	-1.448	-3.794	2.188	2.995	1.335

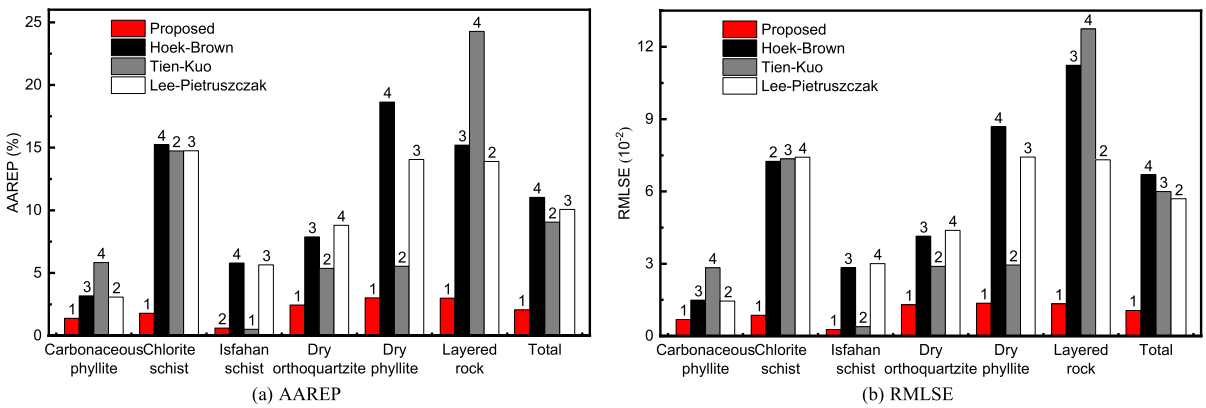

Fig. 6 Error measures of the four empirical relations for m_b values of six jointed rock masses

advantages of the proposed empirical relation, the AAREP and RMLSE of the three existing empirical functions introduced above and the proposed empirical relation are summarized in Fig. 6, and these relations are ranked according to their prediction accuracy.

Because the m_b of carbonaceous phyllite changes slightly with dip angle, these four empirical relations all show good prediction effects, and the proposed empirical relation performs the best. For chlorite schist and dry orthoquartzite, whose m_b variations are similar to the periodic function, the predictions of the proposed empirical relation are markedly better than those of the other three relations. The m_b variation of Isfahan schist is a quadratic function curve symmetrical about $\beta = 45°$; thus, the empirical relationship proposed by Tiankuo performs well, and the empirical relationship established in this paper also achieves good predictions. It can be seen that the proposed empirical relation can accurately predict the periodic and quadratic function curves presented in Fig. 5. For the m_b of all six jointed rock masses, the proposed empirical relation performs markedly better than the existing three empirical relations, and the total AAREP and RMLSE of the established relationship are 2.066% and 1.060×10^{-2}, respectively. The prediction qualities of the other three empirical relations are poor, and the empirical relation established by Hoek and Brown performs the worst.

Based on the constant terms in Table 4, the calculated m_b values of the six jointed rock masses at different β are obtained. By combining Eq. (15), the failure strengths under different pressures σ_3 are estimated. The predicted strength values and test results of each rock type are presented in Fig. 7, and the points closer to the contour line represent a better prediction effect. The predicted values of the six rock types in Fig. 7 are all within the upper/lower limit of 85%, indicating that the predicted results agree well with the test results. Table 4 shows that the proposed empirical relation $m_b(\beta)$ achieves the worst prediction for dry phyllite; thus, the data points in Fig. 7b are scattered, and the predictive ability is reduced.

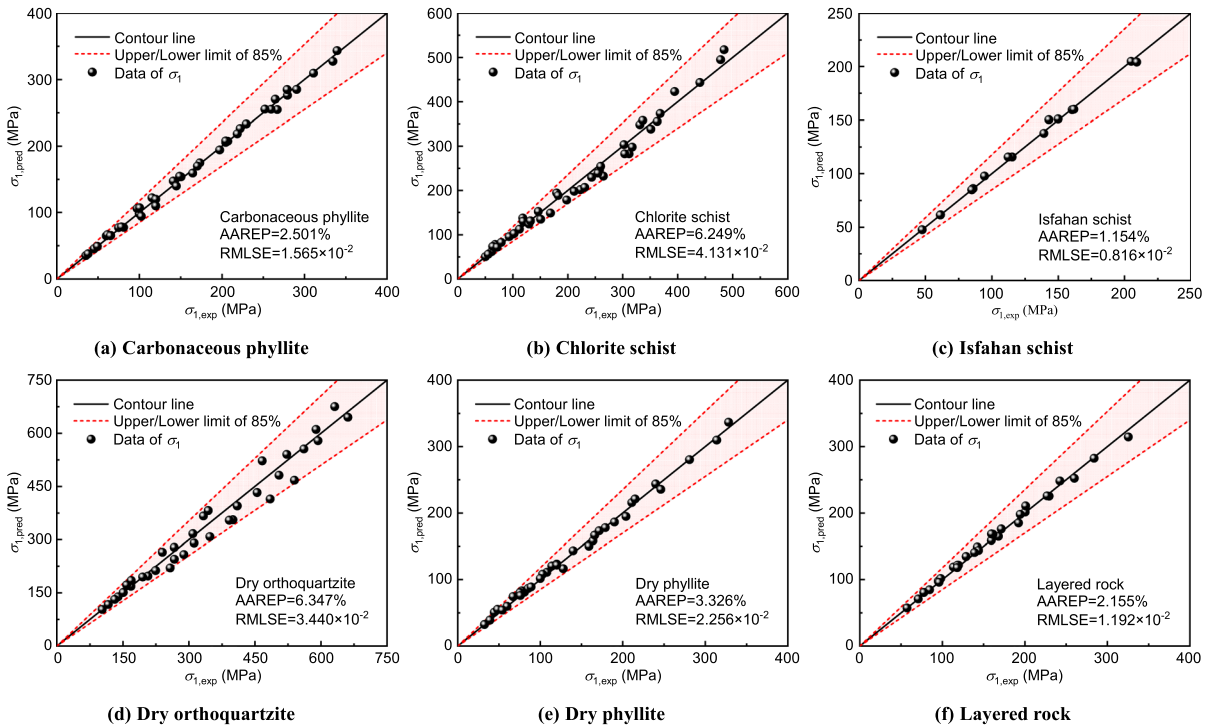

(a) Carbonaceous phyllite **(b) Chlorite schist** **(c) Isfahan schist**

(d) Dry orthoquartzite **(e) Dry phyllite** **(f) Layered rock**

Fig. 7 Comparison between σ_1 values predicted via the proposed 3D HB criterion for jointed rock masses and experimental results

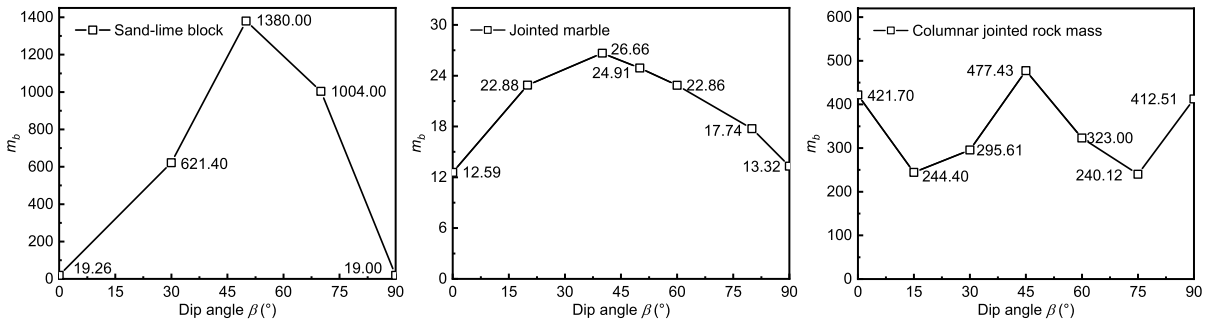

(a) Sand-lime block **(b) Jointed marble** **(c) Columnar jointed rock mass**

Fig. 8 Variation in the m_b value with dip angle β

Table 5 Calibration results of the proposed empirical relation $m_b(\beta)$ for three jointed rock masses

Rock type	A	B	C	w	AAREP (%)	RMLSE (10^{-2})
Sand-lime block	657.898	−644.832	−412.438	3.962	12.856	6.246
Jointed marble	−115,999.869	116,013.132	−1696.994	−0.019	7.334	3.323
Columnar jointed rock mass	344.100	85.860	−84.910	6.898	2.015	0.997

Table 6 Calibration results of the proposed 3D HB criterion for three jointed rock masses

Rock type	Dip angle β (°)	m_b	σ_{cj} (MPa)	n	AAREP (%)	RMLSE (10^{-2})
Sand-lime block	0	13.066	5.681	0.252	5.703	2.872
	30	607.797	0.029	1	14.153	6.411
	50	1398.902	0.046	1	13.028	6.906
	70	984.845	0.061	1	6.280	2.531
	90	39.044	2.560	0.475	4.362	2.089
	Total				8.581	4.595
Jointed marble	0	13.263	157.100	0.338	4.240	2.263
	20	21.904	111.700	0.309	7.056	3.441
	40	25.544	80.930	0.407	6.171	3.003
	50	25.488	74.380	0.406	3.992	1.998
	60	24.182	78.270	0.303	2.879	1.542
	80	17.817	121.700	0.066	6.977	3.156
	90	12.760	159.600	0.007	9.980	4.480
	Total				5.899	2.985
Columnar jointed rock mass	0	429.960	0.078	0	5.130	2.251
	15	241.519	0.122	0	2.394	1.148
	30	306.051	0.093	0.014	2.148	0.896
	45	464.415	0.053	0	5.268	2.767
	60	326.072	0.054	0	13.728	6.311
	75	232.188	0.098	0	8.368	5.682
	90	414.288	0.149	0	5.264	2.657
	Total				5.657	3.380

Overall, the proposed 3D HB criterion for jointed rock masses can effectively estimate the σ_1 values of six jointed rock masses with different β when $\sigma_2 = \sigma_3$.

Then, three true triaxial datasets (Online Resource 3) were used to demonstrate the effectiveness of the proposed empirical relation $m_b(\beta)$ and the 3D HB criterion in evaluating the strength behaviors of jointed rock masses when $\sigma_2 \neq \sigma_3$. The three rock types include the sand-lime block (Tiwari and Rao 2007), jointed marble (Gao et al. 2020), and columnar jointed rock mass (Lu 2021). The data number for sand-lime block, jointed marble and columnar jointed rock mass is 44, 35, and 32, respectively. By fitting Eq. (20) with the test data, the variations in the m_b

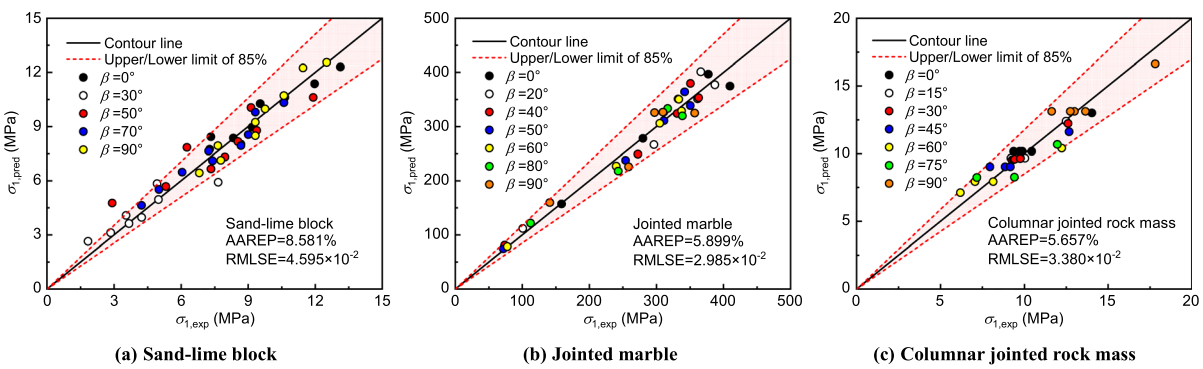

Fig. 9 Comparison between σ_1 values predicted via the proposed 3D HB criterion for jointed rock masses and experimental results

value with the dip angle of the three rock types are shown in Fig. 8.

As shown in Fig. 8, the m_b of the sand-lime block and jointed marble exhibit a quadratic function with β, and the variation curve of the columnar jointed rock is 'W-shaped'. The m_b of the three jointed rock masses are fitted with Eq. (19), and the calculated constant term values and error measures AAREP and RMLSE are listed in Table 5. Overall, the proposed empirical relation $m_b(\beta)$ achieves good predictions of the m_b for the three rock types. The AAREP and RMLSE of the sand-lime block are 12.856% and 6.246×10^{-2}, respectively, indicating relatively poor prediction performance.

The constant term values in Table 5 and Eq. (19) are used to calculate the empirical parameter m_b at different dip angles of the three jointed rock masses, and the calculated values are listed in Table 6. The true triaxial test values are fitted with Eq. (20), and the calculated values of weighting factor n and two error measures are also listed in Table 6. In addition, both the $\sigma_{1,\text{test}}$ and $\sigma_{1,\text{pred}}$ values are plotted in Fig. 9.

According to the error measures shown in Table 6, the proposed criterion achieves the worst predictions of the failure strength of the sand-lime block due to the relatively poor prediction performance of the established $m_b(\beta)$ for m_b. As shown in Fig. 9a, 90.909% of the points are within the error limit, and four points beyond this range correspond to dip angles of 30° and 50°. The sensitivity of the sand-lime blocks at different β to changes in the stress environment varies considerably. In particular, the variation of σ_1 value with confining pressure for blocks with dip angles of 30° and 50° is different from that for blocks with other dip angles. When $\sigma_2=\sigma_3=0.31$ MPa and 0.78 MPa, the failure strengths of 30° and 50° are significantly lower than those of other dip angles. The ratios between the maximum and minimum failure strengths under different confining pressures corresponding to 0°, 70° and 90° are in the range of 1.8–2.5. When $\beta=30°$ and 50°, the data are scattered, and the corresponding ratios are 4.2 and 4.1, respectively. Therefore, the predictions for the strength values of 30° and 50° are worse than those of other dip angles. For jointed marble and columnar jointed rock mass, all $\sigma_{1,\text{pred}}$ values are within the error limit, indicating that the predicted results are consistent with the test values. Overall, the proposed 3D HB strength criterion for jointed rock masses can effectively predict the strength values for different β when $\sigma_2\neq\sigma_3$.

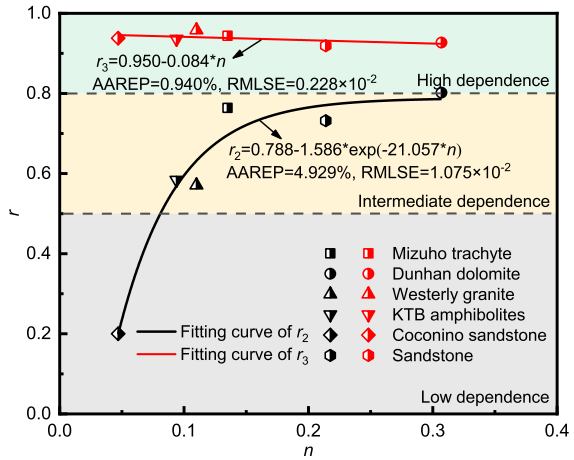

Fig. 10 Relationship between influence coefficient n and partial correlation factor r

4 Discussion

4.1 Physical meaning of weighting factor n

To assess the association between two variables v_1 and v_2, the correlation factor r is typically applied (Freund et al. 2010). The specific expression is

$$r[v_1,v_2]=\frac{Cov[v_1,v_2]}{\sqrt{Var[v_1]\cdot Var[v_2]}} \tag{21}$$

where $Cov[v_1, v_2]$ represents the covariance between v_1 and v_2; $Var[v_1]$ represents the deviation of v_1; and $Var[v_2]$ represents the deviation of v_2. To quantitatively describe the roles of σ_2 and σ_3, the partial correlation factors r_2 and r_3 were introduced (Ma et al. 2020):

$$r_2=r[\sigma_1,\sigma_2:\sigma_3]=\frac{r[\sigma_1,\sigma_2]-r[\sigma_1,\sigma_3]\cdot r[\sigma_2,\sigma_3]}{\sqrt{(1-r^2[\sigma_1,\sigma_3])\cdot(1-r^2[\sigma_2,\sigma_3])}} \tag{22}$$

$$r_3=r[\sigma_1,\sigma_3:\sigma_2]=\frac{r[\sigma_1,\sigma_3]-r[\sigma_1,\sigma_2]\cdot r[\sigma_2,\sigma_3]}{\sqrt{(1-r^2[\sigma_1,\sigma_2])\cdot(1-r^2[\sigma_2,\sigma_3])}} \tag{23}$$

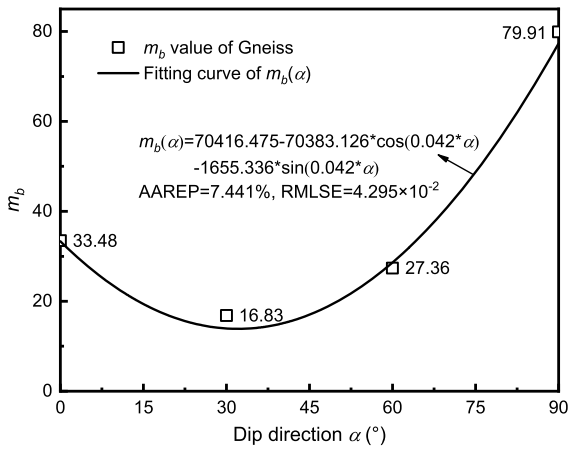

Fig. 11 Variation in the m_b value with dip direction α

where the factors r_2 and r_3 are used to assess the influence of σ_2 and σ_3, respectively. The minimum and maximum absolute values of r_2 and r_3 are 0 and 1, respectively. An absolute value of r_2 or r_3 close to 1 means that the σ_2 or σ_3 has a significant effect on the failure strength.

The partial correlation factors r_2 and r_3 of the six intact rocks in Sect. 2.3 were calculated and compared with the weighting factor n in Table 2. Figure 10 shows the relationships between the weighting factor n in the proposed 3D criterion and the two partial correlation factors. Based on r, the plane is divided into three parts, representing different degrees of stress dependence (Ma et al. 2020).

As shown in Fig. 10, most intact rocks (Mizuho trachyte, westerly granite, KTB amphibolites, Coconino sandstone, and sandstone) exhibit low and intermediate σ_2 dependencies. The partial correlation factor r_2 of the Dunhan dolomite is 0.802, indicating a high σ_2 dependence. The relation between n and r_2 exhibits a clear exponential function, and the partial correlation factor r_2 increases with the weighting factor n. The partial correlation factor r_3 of all intact rocks is greater than 0.8, indicating a high σ_3 dependence. There is a linear relationship between n and r_3, and the partial correlation factor r_3 decreases with the weighting factor n. The weighting factor n in the proposed criterion is closely correlated to the partial correlation factors r_2 and r_3, which means that n can effectively evaluate the roles of σ_2 and σ_3. Meanwhile, it is worth trying to use the calculated partial correlation factors r_2 and r_3 to obtain the weighting factor n.

Table 7 Calibration results of the proposed 3D HB criterion for gneiss with different dip directions α

Dip direction α (°)	m_b	σ_{cj} (MPa)	n	AAREP (%)	RMLSE (10^{-2})
0	33.349	63.720	0.572	6.521	3.433
30	13.728	146.300	1	1.622	0.797
60	28.709	122.600	0.887	3.904	2.088
90	78.284	49.770	1	7.557	4.891
Total				4.901	3.190

4.2 Consideration of dip direction α

The establishment of a true triaxial criterion for jointed rock masses also requires the consideration of joint dip direction α. However, because of the shortage of true triaxial datasets considering both α and β (Feng et al. 2019; Zhang et al. 2012; Zhao et al. 2021), only the inclination angle β is considered in Sect. 2.2. In this section, the dip direction α is considered separately, and the validity of establishing the relationship between m_b and α in the same function form as $m_b(\beta)$ (Eq. (19)) is verified. To discuss the effect of α, the true triaxial dataset of gneiss performed by Liu et al. (2020) were used (Online Resource 4). The number of test data is 16. In this true triaxial compression test, the dip angle β is fixed at 30°, and the dip directions α

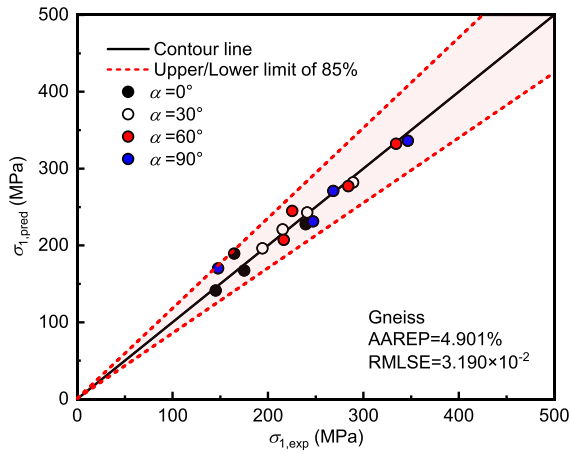

Fig. 12 Comparison between σ_1 values predicted via the proposed 3D HB criterion for gneiss and experimental results

are 0°, 30°, 60°, and 90°. The true triaxial test results are fitted with Eq. (20), and the calculated m_b at different dip directions are summarized in Fig. 11. The m_b corresponding to different dip directions is predicted by a function expression of Eq. (19), and the fitting curve is also plotted in Fig. 11.

As shown in Fig. 11, m_b first drops and then rises with α. The fitting curve agrees well with the data points, and the AAREP and RMLSE are 7.441% and 4.295×10^{-2}, respectively. Table 7 lists the m_b values for different dip directions α calculated from the obtained relation $m_b(\alpha)$. The σ_1 values of gneiss at different dip directions are predicted using the proposed 3D criterion, and the calculated weighting factor n and two error measures are also shown in Table 6. The σ_{cj} values are the uniaxial compression strengths. In addition, the $\sigma_{1,\text{test}}$ and $\sigma_{1,\text{pred}}$ values of gneiss are plotted in Fig. 12.

Table 7 and Fig. 12 demonstrate that the proposed criterion works well in predicting the failure strengths of gneiss at different dip directions, and the AAREP and RMLSE are 4.901% and 3.190×10^{-2}, respectively. All points are within the error limit, indicating that the predicted values agree with the test results; this result demonstrates that the empirical relation $m_b(\alpha)$ in the same form as Eq. (19) can effectively determine the m_b value for different α so that the proposed 3D strength criterion shows good prediction performance.

Strengthening the true triaxial test study of jointed rock masses considering both α and β can effectively improve the 3D strength criterion for jointed rock masses. With sufficient test data, the 3D criterion established in this paper will be promoted. If possible, the following empirical relationship $m_b(\alpha, \beta)$ can provide a reference for studying the effects of α and β simultaneously:

$$m_b(\alpha,\beta) = m_b(\alpha)\cdot m_b(\beta) \tag{24}$$

5 Conclusions

To describe the roles of σ_2 and σ_3 on the strength behaviors of intact rocks, a novel 3D version of the HB criterion was developed. Subsequently, an empirical function $m_b(\beta)$ was established to apply the proposed 3D HB criterion to jointed rock masses. The main conclusions are summarized as follows:

1. The failure envelope of the proposed strength criterion in the π-plane is an irregular hexagon and gradually expands outward as n increases from 0 to 1. When $n=0$, the expression of the proposed version reduces to the original HB criterion, and their envelopes are overlapping. When $n=1$, the expression of the proposed criterion becomes the Singh criterion, and the two envelopes are the same.
2. The proposed criterion and five other existing 3D criteria for intact rocks are validated using six sets of polyaxial test data. Overall, the proposed criterion performs the best, followed by the Priest, Jiang–Zhao, HB, Pan–Hudson, and Singh strength criteria. This is because the proposed criterion can adjust the stress weighting factor n according to the impacts of σ_2 and σ_3 on the rock failure.
3. The m_b of six jointed rock masses at different dip angles β were predicted using the established relationship and three other existing empirical expressions, and the prediction qualities were compared. The proposed empirical relation $m_b(\beta)$ performed markedly better than the other relations; thus, the proposed 3D HB criterion can effectively determine the strength values of these six rock types when $\sigma_2=\sigma_3$.
4. The applicabilities of the proposed empirical relation $m_b(\beta)$ and the modified 3D HB criterion under unequal confining pressures were verified using three true triaxial datasets. Results showed that the established empirical relationship achieves good predictions of the m_b of three jointed rock masses, and the predicted strengths at different dip angles were consistent with the test results.
5. The weighting factor n is closely correlated to the partial correlation factors r_2 and r_3 of principal stress σ_2 and σ_3. The expression of the established relation $m_b(\beta)$ can also be used to accurately describe the variation in m_b with the dip direction α, providing space to develop a better 3D strength criterion for jointed rock masses.

Acknowledgements This work was supported by the Fundamental Research Funds for the Central Universities, the Postgraduate Research & Practice Innovation Program of Jiangsu Province (Grant No. KYCX21_0487), and the National Natural Science Foundation of China (Grant Nos. 41831278, 51878249, and 51579081).

Author contributions All authors contributed to the study conception and design. XQ contributed to data collection, methodology, project administration, funding acquisition, and writing of first draft. ZZ contributed to data curation, funding acquisition, and revision of manuscript. ZN contributed to data curation, conceptualization, and revision of manuscript. SZ and LW contributed to data collection and supervision.

Availability of data and materials All data generated or used during the study are available.

Code availability Not applicable.

Declarations

Ethics approval and consent to participate Not applicable. Informed consent was obtained from all individual participants included in the study.

Consent for publication Consent for publication was obtained from all individual participants included in the study.

Competing interests The authors declare that they have no known competing financial interests or personal relationships that could have appeared to influence the work reported in this paper.

References

Chang C, Haimson B (2000) True triaxial strength and deformability of the German Continental Deep Drilling Program (KTB) deep hole amphibolite. J Geophys Res-Sol Ea 105(B8):18999–19013. https://doi.org/10.1029/2000JB900184

Chen HH, Zhu HH, Zhang LY (2021) A unified constitutive model for rock based on newly modified GZZ criterion. Rock Mechan Rock Eng 54:921–935. https://doi.org/10.1007/s00603-020-02293-y

Colak K, Unlu T (2004) Effect of transverse anisotropy on the Hoek-Brown strength parameter 'm_i' for intact rocks. Int J Rock Mech Min Sci 41:1045–1052. https://doi.org/10.1016/j.ijrmms.2004.04.004

Drucker DC, Prager W (1952) Soil mechanics and plastic analysis or limit design. Q Appl Math 10(2):157–165. https://doi.org/10.1090/qam/48291

Du K, Yang CZ, Su R, Tao M, Wang SF (2020) Failure properties of cubic granite, marble, and sandstone specimens under true triaxial stress. Int J Rock Mech Min Sci 130:104309. https://doi.org/10.1016/j.ijrmms.2020.104309

Fehimifar A (2004) Strength and deformation properties of a schist rock in Isfahan. Iran J Sci Technol B 28(B5):619–622. https://doi.org/10.22099/IJSTC.2013.1114

Feng XT, Zhou YY, Jiang Q (2019) Rock mechanics contributions to recent hydroelectric developments in China. J Rock Mech Geotech Eng 11(3):551–526. https://doi.org/10.1016/j.jrmge.2018.09.006

Freund RJ, Mohr D, Wilson WJ (2010) Statistical methods. Academic Press, London

Gao F, Yang YG, Cheng HM, Cai CZ (2019) Novel 3D failure criterion for rock materials. Int J Geomech 19(6):04019046. https://doi.org/10.1061/(ASCE)GM.1943-5622.0001421

Gao YH, Feng XT, Zhang XW, Feng GL, Jiang Q, Qiu SL (2018) Characteristic stress levels and brittle fracturing of hard rocks subjected to true triaxial compression with low minimum principal stress. Rock Mech Rock Eng 51(12):3681–3697. https://doi.org/10.1007/s00603-018-1548-4

Gao YH, Feng XT, Wang ZF, Zhang XW (2020) Strength and failure characteristics of jointed marble under true triaxial compression. Bull Eng Geol Environ 79(2):891–905. https://doi.org/10.1007/s10064-019-01610-2

Gong B, Wang SY, Sloan SW, Sheng DC, Tang CA (2019) Modelling rock failure with a novel continuous to discontinuous method. Rock Mech Rock Eng 52(9):3183–3195. https://doi.org/10.1007/s00603-019-01754-3

Haimson B, Chang C (2000) A new true triaxial cell for testing mechanical properties of rock, and its use to determine rock strength and deformability of Westerly granite. Int J Rock Mech Min Sci 37(1–2):285–296. https://doi.org/10.1016/S1365-1609(99)00106-9

Hoek E, Brown ET (1980) Underground excavations in rock. CRC Press, London

Hoek E, Wood D, Shah S, Hudson JA (1992) A modified Hoek-Brown criterion for jointed rock masses. Rock Characterization: ISRM Symposium. Thomas Telford Publishing, London, pp 209–214

Ismael M, Konietzky H (2019) Constitutive model for inherent anisotropic rocks: Ubiquitous joint model based on the Hoek-Brown failure criterion. Comput Geotech 105:99–109. https://doi.org/10.1016/j.compgeo.2018.09.016

Jaeger JC (1960) Shear failure of anistropic rocks. Geol Mag 97(1):65–72. https://doi.org/10.1017/S0016756800061100

Jiang H, Zhao JD (2015) A simple three-dimensional failure criterion for rocks based on the Hoek-Brown criterion. Rock Mech Rock Eng 48(5):1807–1819. https://doi.org/10.1007/s00603-014-0691-9

Kumar A (2006) Engineering behaviour of anisotropic rocks. Dissertation, IIT Roorkee, Roorkee

Lee YK, Pietruszczak S (2008) Application of critical plane approach to the prediction of strength anisotropy in transversely isotropic rock masses. Int J Rock Mech Min Sci 45(4):513–523. https://doi.org/10.1016/j.ijrmms.2007.07.017

Li HT, Qi QX, Du WS, Li XP (2022) A criterion of rockburst in coal mines considering the influence of working face mining velocity. Geomech Geophys GeoEnergy GeoResour 8:37. https://doi.org/10.1007/s40948-021-00338-2

Li HZ, Guo T, Nan YL, Han B (2021) A simplified three-dimensional extension of Hoek-Brown strength criterion. J Rock Mech Geotech Eng 13(3):568–578. https://doi.org/10.1016/j.jrmge.2020.10.004

Liu XF, Feng XT, Zhou YY (2020) Experimental study of mechanical behavior of gneiss considering the orientation of schistosity under true triaxial compression. Int J Geomech 20(11):04020199. https://doi.org/10.1061/(ASCE)GM.1943-5622.0001838

Lu WB (2021) Study on true triaxial mechanical test and constitutive model of columnar jointed rock mass. Dissertation, Hohai University

Ma LJ, Li Z, Wang MY, Wu JW, Li G (2020) Applicability of a new modified explicit three-dimensional Hoek-Brown failure criterion to eight rocks. Int J Rock Mech Min Sci 133:104311. https://doi.org/10.1016/j.ijrmms.2020.104311

Ma XD, Haimson BC (2016) Failure characteristics of two porous sandstones subjected to true triaxial stresses. J Geophys Res-Sol Ea 121(9):6477–6498. https://doi.org/10.1002/2016JB012979

Merifield RS, Lyamin AV, Sloan SW (2006) Limit analysis solutions for the bearing capacity of rock masses using the generalised Hoek-Brown criterion. Int J Rock Mech Min Sci 43(6):920–937. https://doi.org/10.1016/j.ijrmms.2006.02.001

Mogi K (1967) Effect of the intermediate principal stress on rock failure. J Geophys Res 72(20):5117–5131. https://doi.org/10.1029/JZ072i020p05117

Mogi K (1971) Fracture and flow of rocks under high triaxial compression. J Geophys Res 76(5):1255–1269. https://doi.org/10.1029/JB076i005p01255

Nasseri MHB, Rao KS, Ramamurthy T (2003) Anisotropic strength and deformational behavior of Himalayan schists. Int J Rock Mech Min Sci 40:3–23. https://doi.org/10.1016/S1365-1609(02)00103-X

Pan XD, Hudson JA (1988) A simplified three dimensional Hoek–Brown yield criterion. In: ISRM International Symposium. OnePetro

Priest SD (2005) Determination of shear strength and three-dimensional yield strength for the Hoek-Brown criterion. Rock Mech Rock Eng 38(4):299–327. https://doi.org/10.1007/s00603-005-0056-5

Saroglou H, Tsiambaos G (2008) A modifified Hoek-Brown failure criterion for anisotropic intact rock. Int J Rock Mech Min Sci 45:223–234. https://doi.org/10.1016/j.ijrmms.2007.05.004

Singh A, Kumar A, Rao KS (2018) Strength behaviour of anisotropic rock under true triaxial stress state. In: ISRM international symposium-10th Asian rock mechanics symposium. OnePetro

Singh B, Goel RK, Mehrotra VK, Garg SK, Allu MR (1998) Effect of intermediate principal stress on strength of anisotropic rock mass. Tunn Undergr Sp Tech 13(1):71–79. https://doi.org/10.1016/S0886-7798(98)00023-6

Singh J, Ramamurthy T, Rao G (1989) Strength anisotropies in rocks. Indian Geotech J 19:147–166

Takahashi M, Koide H (1989) Effect of the intermediate principal stress on strength and deformation behavior of sedimentary rocks at the depth shallower than 2000 m. In: ISRM international symposium. OnePetro

Tien YM, Kuo MC (2001) A failure criterion for transversely isotropic rocks. Int J Rock Mech Min Sci 38(3):399–412. https://doi.org/10.1016/S1365-1609(01)00007-7

Tiwari RP, Rao KS (2007) Response of an anisotropic rock mass under polyaxial stress state. J Mater Civil Eng 19(5):393–403. https://doi.org/10.1061/(ASCE)0899-1561(2007)19:5(393)

Wen T, Tang HM, Huang L, Hamza A, Wang YK (2021) An empirical relation for parameter m_i in the Hoek-Brown criterion of anisotropic intact rocks with consideration of the minor principal stress and stress-to-weak-plane angle. Acta Geotech 16(2):551–567. https://doi.org/10.1007/s11440-020-01039-y

Wu S, Zhang S, Guo C, Xiong L (2017) A generalized nonlinear failure criterion for frictional materials. Acta Geotech 12:1353–1371. https://doi.org/10.1007/s11440-017-0532-6

Yang Q, Zan YW, Xie LG (2018) Comparative analysis of the nonlinear unified strength criterion for rocks and other three-dimensional Hoek-Brown strength criteria. Geomech Geophys GeoEnergy GeoResour 4:29–37. https://doi.org/10.1007/s40948-017-0072-4

Zhang JW, Fan WB, Niu WM, Wang SY (2022) Energy evolution characteristics of deep sandstone with different true triaxial stress paths. Geomech Geophys GeoEnergy GeoResour 8:62. https://doi.org/10.1007/s40948-022-00374-6

Zhang L (2008) A generalized three-dimensional Hoek-Brown strength criterion. Rock Mech Rock Eng 41(6):893–915. https://doi.org/10.1007/s00603-008-0169-8

Zhang YL, Shao JF, Saxcé GD, Shi C, Liu ZB (2019) Study of deformation and failure in an anisotropic rock with a three-dimensional discrete element model. Int J Rock Mech Min Sci 120:17–28. https://doi.org/10.1016/j.ijrmms.2019.05.007

Zhang ZZ, Zhou LL, Yuan ZX, Sun ZH (2012) Research on shear failure criterion for layered rock mass. Adv Mater Res 446:1491–1496. https://doi.org/10.4028/www.scientific.net/AMR.446-449.1491

Zhao WC, Liu Y, Wang TT, Ranjith PG, Zhang YF (2021) Stability analysis of wellbore for multiple weakness planes in shale formations. Geomech Geophys GeoEnergy GeoResour 7:44. https://doi.org/10.1007/s40948-021-00228-7

Zhu QZ, Shao JF (2020) A semi-empirical failure criterion for brittle rocks. Rock Mech Rock Eng 53(9):4271–4277. https://doi.org/10.1007/s00603-020-02125-z

Terms and Conditions

Springer Nature journal content, brought to you courtesy of Springer Nature Customer Service Center GmbH (“Springer Nature”).
Springer Nature supports a reasonable amount of sharing of research papers by authors, subscribers and authorised users (“Users”), for small-scale personal, non-commercial use provided that all copyright, trade and service marks and other proprietary notices are maintained. By accessing, sharing, receiving or otherwise using the Springer Nature journal content you agree to these terms of use (“Terms”). For these purposes, Springer Nature considers academic use (by researchers and students) to be non-commercial.
These Terms are supplementary and will apply in addition to any applicable website terms and conditions, a relevant site licence or a personal subscription. These Terms will prevail over any conflict or ambiguity with regards to the relevant terms, a site licence or a personal subscription (to the extent of the conflict or ambiguity only). For Creative Commons-licensed articles, the terms of the Creative Commons license used will apply.
We collect and use personal data to provide access to the Springer Nature journal content. We may also use these personal data internally within ResearchGate and Springer Nature and as agreed share it, in an anonymised way, for purposes of tracking, analysis and reporting. We will not otherwise disclose your personal data outside the ResearchGate or the Springer Nature group of companies unless we have your permission as detailed in the Privacy Policy.
While Users may use the Springer Nature journal content for small scale, personal non-commercial use, it is important to note that Users may not:

1. use such content for the purpose of providing other users with access on a regular or large scale basis or as a means to circumvent access control;
2. use such content where to do so would be considered a criminal or statutory offence in any jurisdiction, or gives rise to civil liability, or is otherwise unlawful;
3. falsely or misleadingly imply or suggest endorsement, approval , sponsorship, or association unless explicitly agreed to by Springer Nature in writing;
4. use bots or other automated methods to access the content or redirect messages
5. override any security feature or exclusionary protocol; or
6. share the content in order to create substitute for Springer Nature products or services or a systematic database of Springer Nature journal content.

In line with the restriction against commercial use, Springer Nature does not permit the creation of a product or service that creates revenue, royalties, rent or income from our content or its inclusion as part of a paid for service or for other commercial gain. Springer Nature journal content cannot be used for inter-library loans and librarians may not upload Springer Nature journal content on a large scale into their, or any other, institutional repository.
These terms of use are reviewed regularly and may be amended at any time. Springer Nature is not obligated to publish any information or content on this website and may remove it or features or functionality at our sole discretion, at any time with or without notice. Springer Nature may revoke this licence to you at any time and remove access to any copies of the Springer Nature journal content which have been saved.
To the fullest extent permitted by law, Springer Nature makes no warranties, representations or guarantees to Users, either express or implied with respect to the Springer nature journal content and all parties disclaim and waive any implied warranties or warranties imposed by law, including merchantability or fitness for any particular purpose.
Please note that these rights do not automatically extend to content, data or other material published by Springer Nature that may be licensed from third parties.
If you would like to use or distribute our Springer Nature journal content to a wider audience or on a regular basis or in any other manner not expressly permitted by these Terms, please contact Springer Nature at

onlineservice@springernature.com